

Towards Nonlinear Quantum Thermodynamics

Gershon Kurizki¹, Nilakantha Meher^{2*}, Avijit Misra³,
Durga Bhaktavatsala Rao Dasari⁴, Tomas Opatrny⁵

¹Department of Chemical and Biological Physics & AMOS, Weizmann
Institute of Science, Rehovot 7610001, Israel.

^{2*}Department of Physics, SRM University AP, Amaravati 522240,
Andhra Pradesh, India.

³Department of Physics, Indian Institute of Technology (ISM),
Dhanbad, Jharkhand 826004, India.

⁴3. Physikalisches Institut, Center for Applied Quantum Technologies,
University of Stuttgart, Stuttgart, 70569, Germany.

⁵Palacky University, 77146 Olomouc, Czech Republic.

*Corresponding author(s). E-mail(s): nilakantha.meher6@gmail.com;
Contributing authors: gershon.kurizki@weizmann.ac.il;
avijitmisra@iitism.ac.in; d.dasari@pi3.uni-stuttgart.de;
tomas.opatrny@upol.cz;

Abstract

We have recently put forth several schemes of unconventional, nonlinearly-enabled thermodynamic (TD) devices that can operate in either the classical or the quantum domain by transforming thermal-state input in multiple uncorrelated modes into non-gaussian state output in selected modes: a four-mode Kerr-nonlinear interferometer that acts as a heat engine; two coupled Kerr-nonlinear Mach-Zehnder interferometers that act as a phase microscope with unprecedented phase resolution; and a noise sensor that can distinguish between unknown nonlinear quantum processes. These schemes reveal the unique merits of nonlinear TD devices: their ability to act in an autonomous, fully coherent, dissipationless fashion, unlike their conventional counterparts. Here we present the opportunities and challenges facing this new paradigm of nonlinear (NL) quantum and classical TD devices along the following lines: A) Linear versus nonlinear multimode transformations in TD devices: what are the principal distinctions between the two types of transformations? B) Classical versus quantum effects in NL TD devices: what are their main differences? Is quantumness an

advantage or a disadvantage? C) Deterministic methods of achieving giant nonlinearity at the few-photon level via coherent processes, including multiatom-bath interactions which can paradoxically yield NL Hamiltonian effects: their comparison with probabilistic, measurement-based methods that can achieve similar NL effects in the quantum domain.

1 Introduction

The ongoing extension of thermodynamics to the quantum domain [1, 2] has been particularly prominent in the introduction of quantum schemes for thermodynamic (TD) devices such as engines and refrigerators [1–34], diodes and transistors [35–44]. Yet, despite the fact that many of these schemes involve quantum coherence and squeezing [9–15, 27, 45, 46] or quantum cooperativity [16–24], they are all based on *dissipative open systems* [1, 2, 47]. Hence, their TD description disqualifies them from acting as fully quantum mechanical devices that are ruled by unitarity.

Aiming to break away from this established paradigm of TD devices as dissipative open systems, we have recently introduced the concept of nonlinear (NL) thermodynamics in both quantum and classical domains. It is concerned with NL effects on field modes that are fed with thermal noise at the input to TD engines or sensors [48–51]. Since each mode is then in a maximal-entropy, passive state, these input modes are neither work nor information resources [29, 31, 52, 53]. Yet if the modes are coherently transformed/mixed or filtered by NL elements within the device, some of them may become non-thermal and constitute useful TD resources for work production in selected output modes that attain non-passive, non-gaussian states, or for quantum-enhanced sensing, by virtue of the high information these states carry [48–51]. Such NL-filtering thermodynamic (TD) devices are treated here as *non-dissipative and fully coherent* to a good approximation. They obey the second law of thermodynamics [1, 2, 54, 55], which excludes entropy reduction in the overall multimode output as compared to the total input, yet allows energy and entropy reshuffling among the modes, which is essential for the device functionality. Such redistribution is accomplished in these NL devices *autonomously*, without external intervention or control. Importantly, since heat baths are replaced in the conceived NL coherent devices by single-mode fields, the appropriate thermodynamic quantities can be inferred from the output photon statistics (compare with [56, 57]).

Here we briefly survey the principles of NL-filtering, coherent TD devices, focusing on multimode interferometers with NL elements that can act as heat engines or quantum sensors (Sec. 2). We then compare the principles of such devices at the quantum and classical level, elucidating the limitations and advantages of their quantumness (Sec. 3). This article is, however, mostly dedicated to possible methods of achieving the giant nonlinearity required for NL filtering at the few-photon level. These methods are allowed by the present technological state-of-the-art to be fully unitary/coherent, hence deterministic (Sec. 4). Yet, as a substitute for these technically demanding methods, one may use probabilistic, measurement-based methods that are shown to provide a viable alternative (Sec. 5). The discussion (Sec. 6) summarizes the results

and presents an outlook to further developments of the NL-filtering thermodynamic approach.

2 Principles and implementations of NL filtering TD devices

A NL coherent TD device, be it a heat engine or a sensor, is governed in the quantum description by a product of unitary evolution operators that have the schematic form

$$\hat{U} = \hat{U}_{L_{out}} \hat{U}_{NL} \hat{U}_{L_{in}} \quad (1a)$$

The overall transformation of the input state ρ_{in} to the output state is then

$$\rho_{out} = \hat{U} \rho_{in} \hat{U}^\dagger \quad (1b)$$

Here $\hat{U}_{L_{in}}$ and $\hat{U}_{L_{out}}$ stand for the linear transformations of the input block into the output block via coherent multimode mixing, and \hat{U}_{NL} is the multi-mode transformation that is responsible for the NL filtering in the device.

The linear transformation operators, effected by conventional beam splitters and phase shifters, constitute rotations on the Poincare sphere of mode-pair states or distributions [58, 59]. Such linear transformations preserve the gaussian character of the individual-mode states. By contrast, a NL transformation, particularly the two-mode cross-Kerr (CK) transformation

$$\hat{U}_{CK} = e^{i\chi \hat{a}^\dagger \hat{a} \hat{b}^\dagger \hat{b}} \quad (2)$$

that couples the photon-number operators of modes a, b with strength χ , can generally twist and distort the mode-pair phase-space distributions and observables [60–62].

Such NL transformations can render the state of a chosen mode non-gaussian and quantum-correlated/entangled with other modes. The input state of each mode may be taken to be thermal, but it is essential that not all input states be at the same temperature, to ensure the non-passive character of the overall multimode input state: the simplest example that adheres to this condition is an input comprised of empty (zero-temperature) modes along with hot modes. Under this condition, a unitary NL transformation as in Eqs. (1), (2) does not create ergotropy [1, 29], but rather redistributes the entropy and energy among the modes in a manner compatible with the second law, such that the states of chosen modes become non-passive, i.e. acquire ergotropy and hence are capable of work production [29, 52] whereas other modes heat up. In what follows, we briefly illustrate the manifestation of these principles in three generic types of NL filtering TD devices: heat engines, phase estimators and quantum noise sensors.

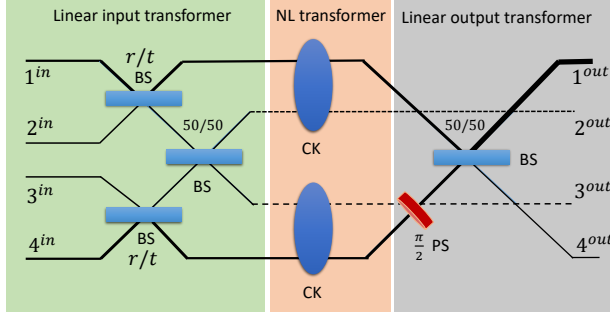


Fig. 1 Nonlinear coherent heat engine. The input contains two hot modes (modes 1^{in} and 4^{in}) and two cold modes (modes 2^{in} and 3^{in}) mixed by linear input transformer. Upon choosing the parameters appropriately, energy is concentrated in mode 1^{out} due to constructive interference between the correlated modes in the NL transformer, followed by steering in a linear output transformer.

2.1 NL- filtering heat engine:

As an example of such an engine, our group analyzed [48] a four-mode interferometer fed by two high-temperature and two zero-temperature (empty) input modes (Fig. 1), modes having the same frequency degenerate. Whereas standard interferometers act as linear transformer that cannot change the output ratio of two modes with equal temperatures, one may control their output ratio upon adding two NL cross-Kerr (CK) elements that create classical correlations or quantum entanglement of all four modes.

One can analyze the resulting NL interference in such a device by viewing the input states in the hot modes 1 and 4 as thermally mixed coherent states that have randomly distributed mean phases and a gaussian distribution of mean amplitudes. For each coherent-state component of these thermal states, the mean intensities in the output (out) modes 1^{out} and 4^{out} , $|\alpha_{1,4}^{out}|^2$, are obtained from their input counterparts by the following relation:

$$|\alpha_{1,4}^{out}|^2 = \frac{r^2}{2} [(\alpha_1^2 + \alpha_4^2)_{in} \pm (\alpha_1 \alpha_4)_{in} \sin(2t^2 \alpha_1 \alpha_4 \chi \cos \phi - \phi)_{in}], \quad (3)$$

Here the CK coupling strength χ is as in Eq. (2), t^2 and r^2 are the respective transmissivity and reflectivity of the input beam-splitter (BS) (see Fig. 1). The interference term in Eq. (3) is non-sinusoidal in the phase difference ϕ of the hot input modes. This term reduces to $\sin \phi$ when $\chi = 0$, resulting in interference washout following averaging over random ϕ . This differs from the case of appreciable CK nonlinearity which gives rise to a narrow-peaked phase ϕ -distribution and, if χ and t are chosen appropriately, causes destructive interference in output mode 4^{out} , and constructive interference in output mode 1^{out} , so that the mean intensity is steered from input mode 4^{in} to output mode 1^{out} . Averaging over random input phases ϕ and a thermal distribution of the hot input modes, yields the following mean intensities (photon

numbers) of the hot output modes satisfy [48]

$$\bar{n}_{1,4}^{out} = r^2 \bar{n} \left[1 \pm \frac{t^2 \chi \bar{n}}{(1 + t^4 \chi^2 \bar{n}^2)^2} \right]. \quad (4)$$

The outcome is then energy amplification in the chosen output mode 1^{out} while the overall energy is conserved. Equally important is the transformation of the input thermal state in mode 1^{in} to a non-passive, non-gaussian state capable of delivering work at the output mode 1^{out} since the NL filtered ergotropy is concentrated in this mode, while entropy increases in all other output modes.

The adherence of this device to the second law of thermodynamics has been verified, analytically and numerically: the analysis shows that the combined four-mode input state is non-passive, although each input mode is in a thermal (passive) state, hence ergotropy is merely redistributed and the sum of entropies of the individual modes increases while the overall entropy is conserved by unitarity (coherent) [48]. This NL-filtering redistribution enables the device to operate as a heat engine capable of coherently transforming heat to work in a designated mode. The extracted work can be measured via power detection resolved at the single-photon level, as has been demonstrated in a superconducting circuit [63].

2.2 NL-filtering thermal quantum sensors:

NL mode couplings have been shown by us [50] to allow supersensitive phase estimation (SSPE) in interferometers illuminated by few photons. Such SSPE can be used in a quantum phase sensor that functions as a transmission microscope. It is based on coupled Mach-Zehnder interferometers (MZIs) in which a sample is detected by means of the phase shift ϕ of radiation transmitted along one of the arms in the MZI (Fig. 2). For classical-like light, the resolvable phase exceeds the standard quantum limit (SQL) [58, 64–66] $\Delta\phi \geq 1/\sqrt{\bar{n}}$. The SQL can, however, be violated by resorting to entangled N00N two-mode states [67] $(|n, 0\rangle + |0, n\rangle)/\sqrt{2}$ comprised of n photons in one mode and 0 in the other, yet these states are hard to implement and easy to destroy by loss and decoherence, particularly for $n \gg 1$.

We pointed out [50] that instead of pure-state N00N input, one may resort to thermal-noise input subject to NL filtering (Fig. 2). The interferometer phase resolution is then much below the SQL and even lower than the nominal Heisenberg uncertainty limit (HL) [58, 64–66] $\Delta\phi \sim 1/\bar{n}$, since the HL does not hold for distributions with small \bar{n} and a large variance, $\Delta n > \bar{n}$, which may allow for $\Delta\phi < 1/\bar{n}$ [59, 68–71].

The phase resolution is limited by the quantum Cramer-Rao bound [72], whereby the minimal phase error that can be reached by a given input state satisfies

$$\Delta\phi_{min} \geq \frac{1}{\sqrt{F_Q}}. \quad (5)$$

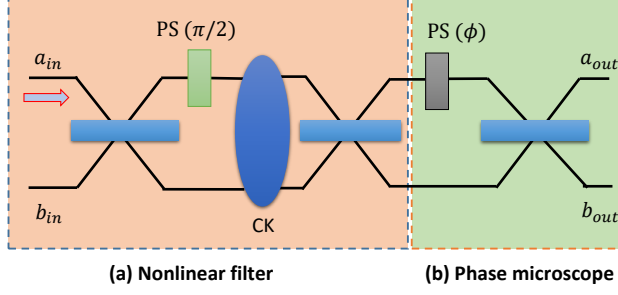


Fig. 2 (a) Nonlinear filter serves as input to (b) transmission microscope aimed at estimating an unknown phase shift (PS) ϕ .

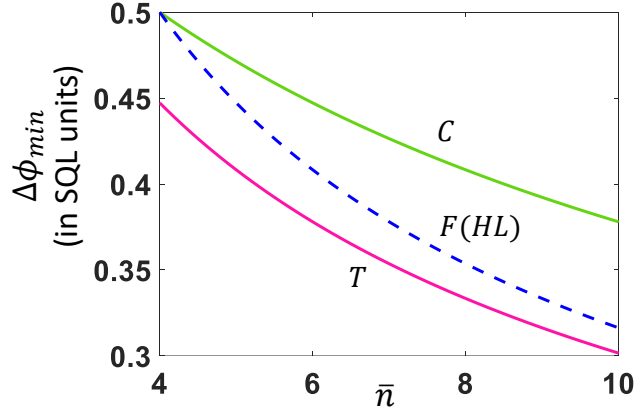


Fig. 3 The minimal phase error normalized to the SQL error as a function of the mean input photon number for thermal (T), coherent (C) and Fock-state (F) inputs to the setup in Fig. 2. Here the CK NL phase shift has the optimal value per photon $\chi = \pi/2$. The F input yields the HL phase error.

F_Q being the quantum Fisher information (QFI) that maximizes the phase-shift estimation accuracy [73]. FQ is determined by the output state of the coupled MZI as in Fig. 2, whose general form is as in Eq. (1b), upon allowing for \hat{U}_{NL} and the phase shift (PS) operation $\hat{U}_{PS}(\phi) = e^{i\phi\hat{a}^\dagger\hat{a}}$ that corresponds to the unknown phase shift ϕ in mode a . In a coupled MZI with cross-Kerr (CK) nonlinearity, $\hat{U}_{NL} = \hat{U}_{CK}$, as in Eq. (2). The CK evolution operator is responsible for the NL filtering in this device.

We have obtained solutions for F_Q corresponding to thermal (T), coherent (C) and Fock-state (F) inputs that are NL- filtered by this coupled MZI, provided the mean input photon number \bar{n} exceeds 4 (Fig. 3)

$$(F_Q)_T = \bar{n}^2 + \bar{n} > (F_Q)_F = \bar{n}^2 > (F_Q)_C = \frac{1}{2}\bar{n}^2 + 2\bar{n}. \quad (6)$$

This surprising result shows that thermal-noise input filtered by the NL(CK) transformation allows higher phase sensitivity than that obtainable through the same NL filtering using Fock- or coherent-state input having equal mean photon numbers [Fig.

3]. This surprising advantage of thermal input has the following reason: the broad Fock state distribution of thermal noise is NL-transformed to a wider distribution of N00N states than its Fock- or coherent-state counterparts, and since the phase sensitivity bound is determined from the quantum Fisher information (QFI) by the highest N00N state, the broadest spread yields the phase resolution.

This finding opens a new path to SSPE using thermal light sources. Remarkably, this SSPE persists even in the presence of high losses in the coupled MZI setup [50].

2.3 NL quantum noise sensors:

NL MZIs endow thermal input in certain modes with information content that may be employed to characterize the Hamiltonian that governs the “black box” medium [74] inside the MZI. This unknown Hamiltonian [75, 76] gives rise to k -photon interaction between the MZI modes, and have, e.g., the form

$$\hat{U}_{NL}^{(k)} = e^{-igt(\hat{a}^{\dagger k} \hat{b}^k + \hat{a}^k \hat{b}^{\dagger k})}, \quad (7)$$

with unknown two-mode coupling strength g , as well as unknown NL-order k .

We have shown [49] that instead of time-consuming tomography [74–78] as a means of characterizing this quantum NL interaction, it may be inferred from the time-dependent ergotropy/ work capacity of an output mode that has been transformed from a gaussian, passive input state to a non-passive, non-gaussian, output state. Importantly, ergotropy does not arise if the underlying noise in the MZI is caused by linear or Raman two-mode coupling, given that the input in each mode is in a thermal, or, more generally, passive, state [1, 29, 52, 79].

Our proposed NL quantum noise sensor illustrates the vast potential of NL filtering: it allows, by single-mode ergotropy probing, to fully characterize unknown two-mode quantum noise properties.

3 Quantum versus classical NL filtering

The foregoing survey attests to the possible advantageous effects and applications of NL-filtered thermal noise whose quantum and classical principles have been briefly outlined above. Here we ask: which of the NL filtering effects are exclusively quantum? By contrast, which effects can be both quantum and classical? What are the advantages or disadvantages of operating in the quantum domain?

We first address these questions in the context of our 4-mode heat engine (Sec. 2). Quantum correlations of the NL-filtered 4-mode fields are rendered by the Stokes operators [80, 81] which can be expressed in terms of the creation and annihilation operators of mode -pair i and j , as $\hat{\mathcal{J}}_+^{(ij)} = \hat{a}_i^\dagger \hat{a}_j$, $\hat{\mathcal{J}}_-^{(ij)} = \hat{a}_i \hat{a}_j^\dagger$, $\hat{\mathcal{J}}_z^{(ij)} = \frac{1}{2}(\hat{a}_i^\dagger \hat{a}_i - \hat{a}_j^\dagger \hat{a}_j)$, $\hat{\mathcal{J}}_0^{(ij)} = \frac{1}{2}(\hat{a}_i^\dagger \hat{a}_i + \hat{a}_j^\dagger \hat{a}_j)$. Under NL transformations, these Stokes operators undergo non-Gaussian twisting that entangles all 4 modes and creates complicated quantum correlated states [60–62].

Classical stochastic mode correlations are described by the ensemble-averaged Stokes parameters, which are the mean values of the Stokes operators described above.

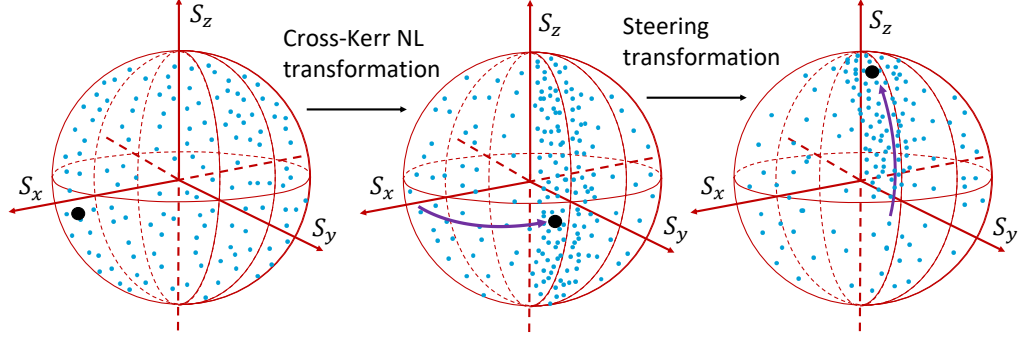


Fig. 4 NL transformation in phase space: Dots denote coherent states that are randomly distributed on the Poincare sphere in the thermal ensemble. The black point denotes a randomly picked state. The violet arrows denote the dots concentration by NL CK (middle) and linear steering by BS and PS (right).

For the hot output modes 1^{out} and 4^{out} , $S_k = \langle \hat{\mathcal{J}}_k^{(14)} \rangle$, $k = x, y, z, 0$. Since a two-mode coherent state corresponds to a point on the surface of the Poincare sphere, their random gaussian distribution in a thermal-ensemble is merely rotated on the sphere surface by linear gaussian operations. By contrast, the NL CK coupler deforms and concentrates the random phase-space distribution in the $S_y < 0$ region of the sphere surface (Fig. 4). This distribution can be subsequently steered by further linear operations to the $S_z > 0$ part of the sphere surface, which corresponds to the mean energy amplification in a chosen mode (here mode 1^{out}). Concurrently, entropy is reduced and ergotropy, that is the capacity for work production [1, 29, 52, 79], is increased in that mode. These redistributions satisfy the first and second laws of thermodynamics in the closed 4-mode system, since the mean-energy is steered to the chosen mode (here from mode 4^{in} to mode 1^{out}) and the entropy reduction in that mode comes at the expense of entropy growth in the undesirable modes (here modes 2 and 3).

In order to compare the above classical and quantum descriptions, let us first assume that the input modes 1^{in} and 4^{in} are populated by coherent states with equal mean amplitudes, $\alpha_1 = \alpha_4$, and random mean phases. The mean quanta numbers in the corresponding output modes, upon averaging over these random phases, are then obtained from a quantum calculation in the form [48]

$$\overline{\langle \hat{n}_{1,4}^{out} \rangle} = \bar{S}_0^{(out)} \pm \bar{S}_z^{(out)} = r^2 \alpha_1^2 (1 \pm J_1(b) e^{-d}). \quad (8)$$

Here $\hat{n}_i = \hat{a}_i^\dagger \hat{a}_i$, $d = t^2(1 - \cos \chi)(\alpha_1^2 + \alpha_4^2)$ and $J_1(b)$ is the first-order Bessel function with argument $b = 2t^2 \alpha_1 \alpha_4 \sin \chi$.

In the corresponding classical calculation [48], Eq. (8) is revised to have $d = 0$. Thus, we find a disadvantage of the quantum NL transformation compared to its classical counterpart: the nonzero d value, which stems from vacuum fluctuations of

the fields in the quantum description, exponentially decreases the energy steering in Eq. (8).

On the other hand, quantum calculations have the unique advantage of allowing us to monitor the changes in the input photon statistics caused by NL transformation effects, which underlie the applications discussed in Sec. 2, particularly the ability to improve phase estimation [50] and sense quantum noise via output-mode ergotropy [49].

Thus, whereas NL-filtered mean-energy flow between modes may feature quantum disadvantage, as illustrated above, there is no substitute for quantumness in applications based on NL transformations of input quantum-statistics: these strictly quantum transformations may endow selected modes with ergotropy and increased information content at the expense of other, unused, modes.

4 Methods of deterministic NL filtering in the quantum domain

Progress towards NL quantum thermodynamics is contingent on the realization of NL effects at the level of a few photons. Two possible giant NL effects are discussed in what follows:

4.1 Dipole-dipole interactions of Rydberg polaritons:

A giant NL CK effect, which was previously predicted by our group [82], has been lately demonstrated [83] in a cold rubidium trap, where each photon is converted by a pump field into a Rydberg atom polariton. In this setup, counter-propagating photon pairs become cross-correlated via dipole-dipole interactions over distances of the order of the photon wavelength [82, 83]. These long-range interactions gives rise to CK phase shifts of π per photon. Thus Rydberg polaritons can be strong enough to impose NL transformations on few-photon thermal states.

4.2 NL multiatom transformations by linear coupling to a thermal bath:

Bath-mediated, dispersive interaction among multiple spins or atoms has been shown by our group [84] to result in an effectively unitary NL state transformation, even though the multispin/multiatom system-bath interaction is linear, as usual. This NL unitary evolution can yield, with high probability, entangled, non-gaussian states, particularly macroscopic quantum superposition (MQS) states, of N atoms or spins that are collectively coupled to a bosonic bath, even if the bath is at finite temperature.

The scenario involves N two-level systems (TLS) that interact with a bosonic (photonic or phononic) bath. It is governed by the collective many-body Hamiltonian

$$\begin{aligned}\hat{H} &= \hat{H}_S + \hat{H}_B + \hat{H}_I, & \hat{H}_S &= \omega_x \hat{J}_x, \\ \hat{H}_B &= \sum_k \omega_k \hat{b}_k^\dagger \hat{b}_k, & \hat{H}_I &= \hat{J}_z \sum_k \eta_k (\hat{b}_k^\dagger + \hat{b}_k).\end{aligned}\tag{9}$$

Here \hat{H}_S, \hat{H}_B and \hat{H}_I are respectively the system, bath, and interaction Hamiltonians, \hat{b}_k^\dagger and \hat{b}_k are the creation and annihilation operators of the k th mode of the bath (B), and η_k are the coupling rates of this mode to the system, all η_k taken to be equal. The collective spin operators in Eq. (9), $\hat{J}_i = \sum_k \hat{\sigma}_k^i$ ($i = x, y, z$), the Cartesian components of the total angular momentum \vec{J} which is the sum of the Pauli operators of the system, $\hat{\sigma}_i^k$ being the Pauli operators for the k th TLS. The total Hamiltonian \hat{H} commutes with $\hat{J}^2 = \sum_i \hat{J}_i^2$, hence the bath couples independently to each subspace of the system that has the total angular-momentum value j , which ranges from 0 to $N/2$.

In order to bypass the intractable effect of noncommutativity of \hat{J}_x and \hat{J}_z in the total Hamiltonian, we switch off the TLS level-splitting ω_x , thereby eliminating \hat{H}_S . The dynamics is then exactly solvable for any bosonic bath. For each j , the joint evolution operator of the system and the bath is then given by

$$\hat{U}_j(t) = \exp \left[-it\Delta_L \hat{J}_z^2 + \hat{J}_z \sum_k \left[\alpha_k(t) \hat{b}_k^\dagger - \alpha_k^*(t) \hat{b}_k \right] \right] \quad (10)$$

where the bath-dependent functions are

$$\begin{aligned} \Delta_L(t) &= \frac{1}{t} \sum_k \eta_k^2 (\omega_k t - \sin \omega_k t) / \omega_k^2, \\ \alpha_k(t) &= \eta_k \frac{1 - e^{i\omega_k t}}{\omega_k} \end{aligned} \quad (11)$$

One thus arrives at a remarkable result: The bath-induced evolution is driven by both linear \hat{J}_z and NL \hat{J}_z^2 operators. While the linear operator gives rise to pure dephasing, the NL operator \hat{J}_z^2 entangles multispin systems. Its effect is a collective bath-induced Lamb shift $\Delta_L(t)$ [85], namely, energy shifting of each spin by all others via virtual-quanta exchange with the bath.

Let us assume that each TLS is initially in a superposition of its energy ($\hat{\sigma}_z^k$) eigenstates. The entire N -spin system then in a product of such superposition states, wherein the individual TLS are *uncorrelated*, which has the form

$$\begin{aligned} \rho(0) &= |\varphi(0)\rangle \langle \varphi(0)|, \\ |\varphi(0)\rangle &= |\theta, \phi\rangle = |\varphi_1\rangle \otimes |\varphi_2\rangle \cdots |\varphi_N\rangle, \\ |\varphi_k\rangle &= \cos \frac{\theta}{2} |\uparrow\rangle + \sin \frac{\theta}{2} e^{i\phi} |\downarrow\rangle. \end{aligned} \quad (12)$$

This state is an eigenstate of the total angular-momentum/spin operator $\vec{J} \cdot \hat{n}$, \hat{n} being the unit vector on the hypersphere defined by the angles θ, ϕ . The decoherence rate $\Gamma(t)$ is made negligible by dynamical control [84], then the NL term $\Delta_L(t) \hat{J}_z^2$ in Eq. (10) evolves the initial uncorrelated state (12) analogously to its evolution under the NL Kerr Hamiltonian [60, 86], into an entangled multipartite state, which attains a non-gaussian form, becoming a macroscopic quantum superposition (MQS) state in due time.

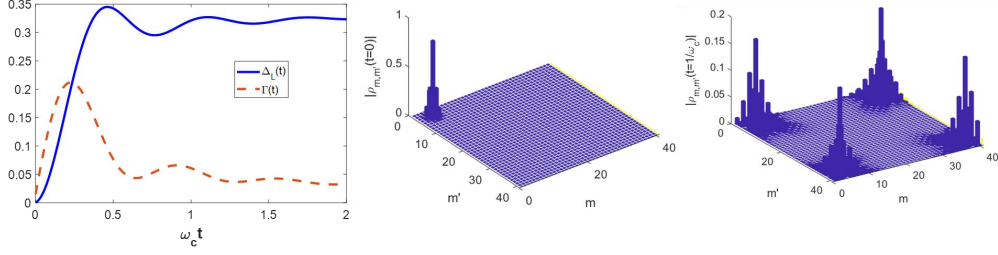


Fig. 5 Multiatom interaction with a cavity-field mode that has a Lorentzian coupling spectrum of width ω_c and centered at ω_0 . Left: $\Delta_L(t)$ and $\Gamma(t)$ are plotted as a function of time. Right: The formation of the macroscopic superposition state at times $t \sim 1/\omega_c$. For the simulations we have chosen $\omega_c/\omega_0 = 10$ and the number of atoms $N = 20$.

The earliest formation time of MQS is then [84]

$$\tau_{MQS} \equiv t = \frac{\pi}{2\Delta_L(t)}. \quad (13)$$

The time at which such a state forms is independent of N and may be much shorter than the decoherence (dephasing) time. This MQS is equivalent to a GHZ-like state in which all the N spins are maximally entangled.

A possible realization of this effect is by N atoms coupled to a leaky cavity bath [87, 88] consisting of photonic modes. Their \hat{J}_x coupling to this bath causes population exchange between the TLS levels or their relaxation and hampers the NL evolution. To overcome this hurdle, we have to eliminate the TLS level splitting, i.e. set $\omega_z = 0$, e.g., by imposing Zeeman shifts. Once the TLS are prepared in degenerate states ($\hat{H}_S = 0$), cooperative coupling can be induced between the cavity bath and the multiatomic system by a Raman process and trigger the collective NL evolution as per Eqs. (10),(11).

The maximal number N of atoms or spins in the MQS is set by the decoherence (dephasing) that depends on the spectral response and the temperature of the bath. A leaky cavity acts as a Lorentzian bath whose decoherence rate may be suppressed by dynamical control that is optimally adapted to the bath spectrum [89]. Nevertheless, the residual decoherence and its finite ratio to the achievable atom-cavity coupling strengths [90–92] may limit the size of the MQS allowed by condition $\tau_{MQS}\bar{\Gamma}N^2 < 1$ to $N < 100$ (Fig. 5), where $\bar{\Gamma}N^2$ is the upper limit of time-averaged decay rate.

Finally, by extending the analysis to 3-level (Lambda) atoms in the cavity, we can map the multiatom MQS to a corresponding entangled state of a two-mode field described by Stokes operators: Under electromagnetically-induced transparency (EIT) conditions in the cavity, the mapping is described by the effective Hamiltonian [93]

$$\hat{H} = g_{eff} \vec{J} \cdot \vec{S}. \quad (14)$$

Here, \vec{J} and \vec{S} are, respectively, the multiatom angular-momentum and the photonic two-mode Stokes operator, effectively coupled with strength g_{eff} .

The exactly solvable model surveyed above reveals the unexpected entangling dynamics of a multiatom or multispin system by a thermal bosonic bath to which it is linearly, collectively coupled. This intriguing consequence of a commonly occurring interaction of a quantum system with a finite-temperature environment may induce the deterministic formation of entangled, non-gaussian, possibly MQS states of the system. These states may then be mapped onto a two-mode photonic MQS of a field incident on the cavity.

If the incident field is thermal, the MQS will be averaged over the thermal distribution in the coherent-state basis. This would hamper but not necessarily destroy the MQS, provided the thermal distribution width is smaller than the decoherence rate of the cavity bath.

It follows from the above discussion that the multiatom interaction with the cavity bath can become an *entangling* resource for initially uncorrelated (unentangled) atoms and (subsequently) two-mode fields. Despite the technical complexity, this approach appears to be a viable route to NL quantum thermodynamics.

5 From deterministic to probabilistic NL transformations

Thus far, we have described deterministic, autonomous NL transformations or filtering of thermal noise to non-gaussian states with advantageous properties: ergotropy for heat engines or information for quantum sensing and microscopy. The open question is: what practical schemes can be made available for the implementation of such NL transformations in the few-photon domain beyond the technically demanding (albeit feasible) schemes discussed in Sec. 4 ?

Alternatively, NL-transformed states can be obtained via the system measurements by a quantum probe, which is coupled to the system by a simple interaction Hamiltonian. Post-selected events, known as conditional measurements (CMs), can prepare the targeted states with limited success probability, which can be optimized.

In the quest for promising measurement-based schemes for NL thermal state transformations, we may be motivated by the recent experimental demonstration that thermal state of a spin bath can be filtered into nearly-pure states by a series of CMs [94] performed on a probe spin coupled to the spin bath. The time-intervals between probe measurements chosen such that the excitation swap of the spin bath and the probe was maximal, conforming to the anti-Zeno (AZE) regime [1, 95]. Only those measurement outcomes were post-selected wherein the swap occurred, to which only spins with certain frequencies contributed. We thus collapsed/filtered the thermal-spin bath state to a nearly pure collective state. Another measurement-based scheme proposed by our group has been recently demonstrated as a probe of single-photon polarization- noise correlations [96].

Can one realize analogous methods to achieve NL filtering of multiphoton noise? In what follows, we highlight several prospective measurement schemes for photonic

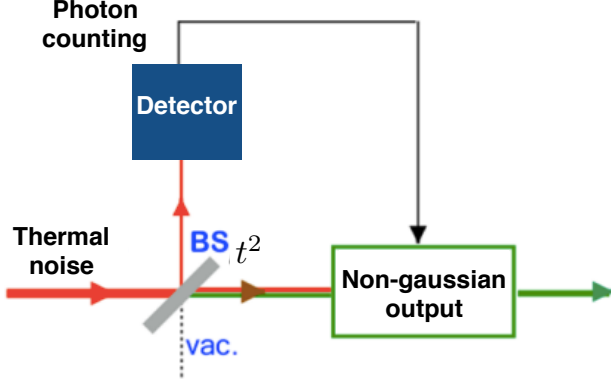


Fig. 6 NL transformation of thermal input by photocount on a small fraction of a noisy input signal reflected by a BS with high transmissivity t^2 .

thermal-state filtering aimed at realizing non-gaussian photon states, particularly Fock states.

5.1 NL transformations of a field mode via photodetection:

NL transformation of a field mode in a thermal state can be achieved by photon counting on a small fraction of the input field, which constitutes a CM of the field state in the Fock basis [97]. The measured small fraction is the reflected part (Fig. 6) of the input beam incident on a BS with high transmissivity t^2 .

The detection of k photons in the reflected fraction yields the measurement-transformed field state which is transmitted through the BS

$$\rho_k = \sum_{n=0}^{\infty} P(n|k) |n\rangle \langle n|. \quad (15)$$

The non-thermal measurement-transformed output state depends on \bar{n} , t^2 and the CM outcome k (Fig. 7). The projection of the reflected beam on the k -photon state is described in the x - p plane by a ring that cuts out a hollow from the gaussian distribution of the input state (Fig. 8). The nonmonotonic character of this ring-shaped outcome state is an evidence of its nonpassivity. Namely, the state in Eq. (15) is passive, by definition, iff the the Fock state populations obey the monotonic falloff as a function of n [29]

$$P(n|k) \geq P(n'|k), \quad \forall n, n', \quad (16)$$

but this condition is violated for $k \neq 0$ measurement results. The corresponding output state is found to be nonthermal upon examining the second-order coherence (autocorrelation) function [64–66] of the state in Eq. (15), which has the form

$$\begin{aligned} g^{(2)}(0) &= \frac{\sum_n P(n|k) n(n-1)}{\bar{n}_k^2} \\ &= 1 + \frac{1}{1+k}. \end{aligned} \quad (17)$$

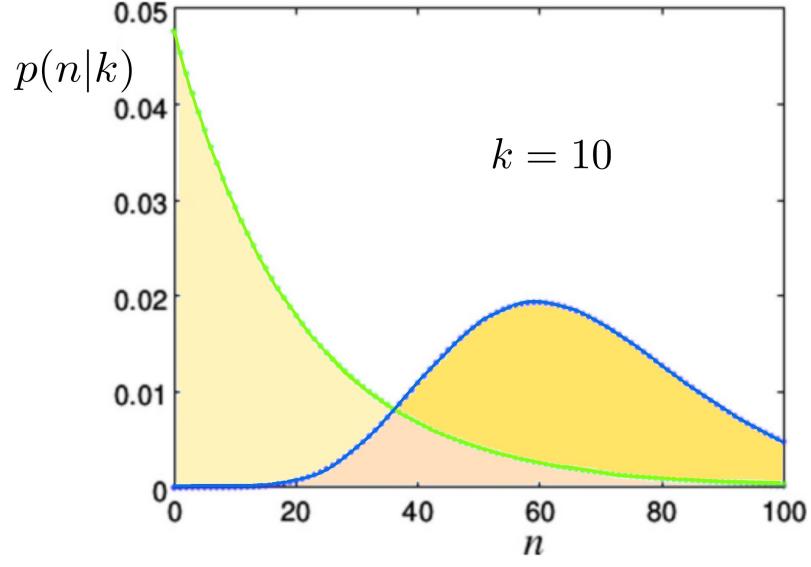


Fig. 7 Fock state distribution in the postmeasured output state for $k = 10$ photon detection. The input thermal state has mean number of photon $\bar{n} = 20$. BS has transmissivity $t^2 = 0.9$. The green and the blue dotted lines represent the initial thermal and postmeasured Fock state distribution respectively.

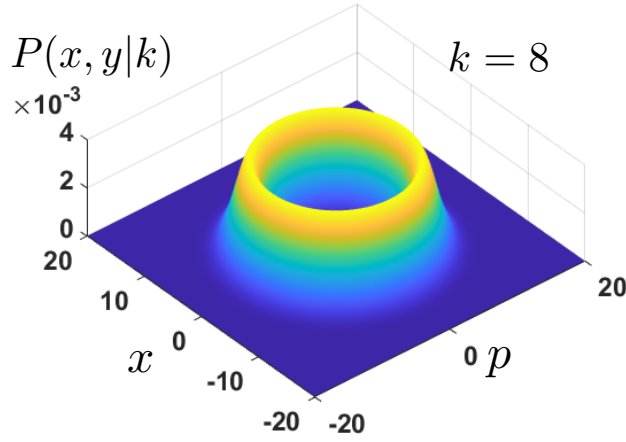


Fig. 8 The phase-plane probability distribution of the output state conditioned on measuring $k = 10$ photons for a thermal input state having $\bar{n} = 20$ and BS transmissivity $t^2 = 0.9$. The nonmonotonic character of the phase-space output distribution corresponds to a non-gaussian, non-passive state.

This expression does not depend on the thermal input temperature or the BS splitting ratio. Only when $k = 0$ photons are counted, the entire beam is transmitted through the BS in a thermal state, with $g^{(2)}(0) = 2$. In the opposite limit of many detected photons, $k \gg 1$, Eq. 17 approaches $g^{(2)}(0) = 1$, corresponding to a Poissonian distribution.

The average energy of the post-measured output state,

$$E_k = \hbar\omega \frac{(1+k)t^2}{e^{\frac{\hbar\omega}{k_B T}} - t^2} \quad (18)$$

can yield the following ergotropy (work capacity) after subtracting the passive part of the output,

$$W_k = E_k - E'_k. \quad (19)$$

Averaging over all possible measurement results k yields the extractable mean work output

$$\bar{W} = \sum_k P_k W_k, \quad (20)$$

which signifies the non-passivity of the overall CM-transformation.

5.2 NL transformations of a field mode via homodyne measurements

Homodyne phase-sensitive measurement of a small reflected fraction constitutes a highly effective CM transformation of a thermal input state [98]. Let us first consider in Fig. 9 a weak input signal in a coherent state $|\alpha\rangle$ with amplitude $\alpha = \frac{1}{\sqrt{2}}(x + ip)$. It is weakly reflected by a BS towards a homodyne-measurement setup where its quadratures are combined with those of local oscillators (LO) with real coherent quadrature-amplitude β and imaginary quadrature amplitude $i\beta$. The two homodyne detectors that measure the orthogonal quadratures of the signal combined with the LO yield photocount differences n_x and n_p which provide information on the input-field quadratures x and p [62].

The same setup can be used to transform a thermal input state with a mean number of photons \bar{n} , which can be represented as a *random mixture of coherent states* $|\alpha\rangle$ with a gaussian P-distribution. The post-measured distribution of α , $P(\alpha|\Delta n_x, \Delta n_p)$ is conditioned on the detection of photon-number differences Δn_x and Δn_p yielding the output state (Fig. 10)

$$\hat{\rho}(\Delta n_x, \Delta n_p) = \frac{1}{t^2} \iint P\left(\frac{\alpha}{t}|\Delta n_x, \Delta n_p\right) |\alpha\rangle\langle\alpha| d^2\alpha \quad (21)$$

The mean work output is obtainable upon averaging the ergotropy over all possible Δn_x , Δn_p and subtracting the energy of the two LOs, $2\hbar\omega\beta^2$. The expression can be optimized with respect to the LO amplitude and the BS transmissivity resulting in the maximal work extractable from the post-measured output is for a thermal state

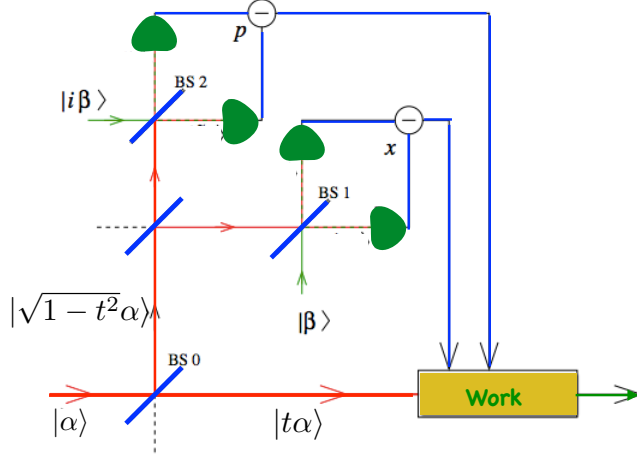


Fig. 9 Homodyne measurement of a small fraction (reflected at BS0) of input state $|\alpha\rangle$. It is mixed with LO quadratures $|\beta\rangle$ and $|i\beta\rangle$ at homodyne setups that measure Δn_x and Δn_p . The postmeasured output (transmitted at BS0) is generally non-passive and can deliver work.

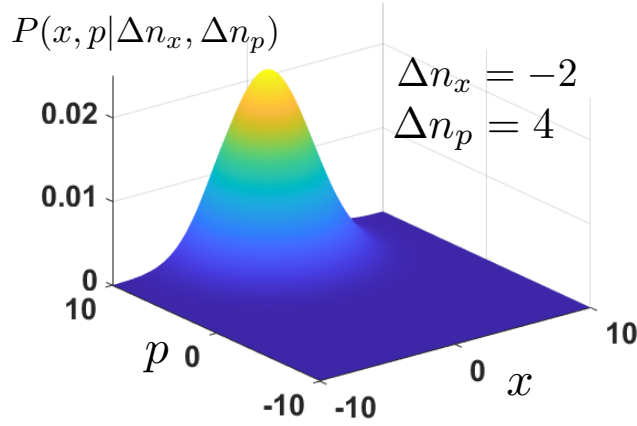


Fig. 10 The phase-space probability distribution of an homodyne measured output state conditioned on homodyne measurement results Δn_x and Δn_p for thermal input state having $\bar{n} = 25$, BS transmissivity $t^2 = 0.8$, and LO mean amplitude $\beta = 1.6$.

with large \bar{n} , the optimized BS transmissivity and LO energy are $1 - t^2 = \frac{1}{\sqrt{\bar{n}}}$ and $2\beta^2 = \sqrt{\bar{n}}$, respectively, yielding the maximal extractable work (in $\hbar\omega$ units) [98]

$$W_{\max} \approx \bar{n} - 4\sqrt{\bar{n}} + 6. \quad (22)$$

The information gain in this small-fraction homodyne transformation is characterized by the mutual information [99, 100] that has to be processed for work extraction via CM feedforward. For maximum work extraction as in Eq. (22), we obtain in the

limit $n \gg 1$ the total mean mutual information gain

$$\mathcal{I} \approx \frac{1}{2} \ln \frac{\bar{n}}{4}. \quad (23)$$

Hence, the cost of feedforward required for work extraction via CM based on the information gained (Eq. 23) becomes negligible compared to output (Eq. 22) for large \bar{n} . This is the main advantage of work extraction obtained by measuring a small fraction of the input, either by photocount or by homodyning (compare with [100]). In any case, the P-distribution of the post-measured state is non-thermal, unless both n_x and n_p are measured to be zero. These measured results control the character of the output state.

Finally, if the results of the measurements discussed above are unread, namely, we resort to nonselective measurements (NSMs) [1, 101], the output state can be shown to remain passive and yield no work, neither via small-fraction homodyne detection nor via small-fraction photodetection [97]. Nevertheless, NSMs that are executed by operators that are capable of extracting work [102, 103].

Remarkably, when the modes are nonlinearly correlated, NSMs can yield work from the intermode correlation energy [104, 105], an effect that goes beyond Landauer's principle [106].

Thus, measurements can transform thermal input states into an ergotropy/work-capacity resource.

5.3 NL transformation of thermal cavity fields by measurements on resonant atoms

Early on, we showed that CMs of the atomic state can yield, on demand, diverse states of a cavity-field mode that is coupled to the atoms, if this field mode initialized in a thermal [107] or coherent state [108–110]. This procedure could be realized by multiple two-level atoms transmitted through an ultrahigh-Q cavity, where they interact with the single-mode field via the resonant Jaynes-Cummings Hamiltonian [66, 85, 90, 92] or its off-resonant (dispersive) [58] variant. Control of the output cavity field state was shown to be enabled in these schemes by adjusting the time-intervals between consecutive atoms in the cavity. This measurement strategy can transform thermal input photon distributions into any chosen Fock state with up to a few tens of photons. Such transformation requires in this strategy can be accomplished in a time that is much shorter than the lifetime of the prepared Fock state.

The strategy is based on intermittent, alternating, application of two types of manipulations:

1. Nonselective measurements (NSMs): We excite the atom and send it through the cavity at a fixed velocity. The atom-field interaction, followed by a NSM on the atom, which amounts to disregarding the measured outcome, following transformation of the number (Fock-) state populations in the cavity

$$\rho_{nn} \rightarrow \rho_{nn} \cos^2(g\tau\sqrt{n+1}) + \rho_{n-1,n-1} \sin^2(g\tau\sqrt{n}), \quad (24)$$

τ being the cavity traversal time, and g the field-atom coupling constant.

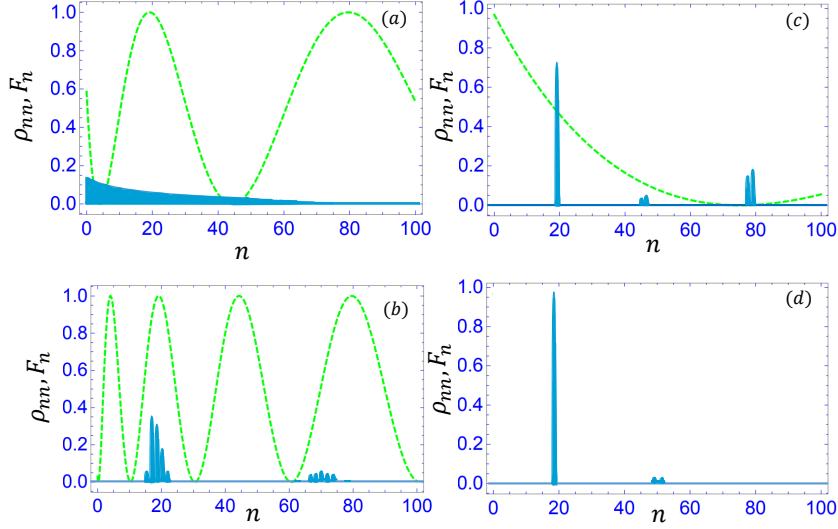


Fig. 11 Evolution of an initial thermal photon-number distribution ρ_{nn} in a cavity towards a target Fock state n via non-selective and conditional measurements (NSM and CM) of initially excited atoms governed by the resonant Jaynes-Cummings interaction Hamiltonian. Dashed green: NSM filter function $\cos^2(g\tau\sqrt{n+1})$ where g and τ are the field-atom coupling strength and interaction time, respectively. Solid blue: ρ_{nn} distribution; (a) Initial ρ_{nn} (b) ρ_{nn} after 100 NSMs for τ_1 chosen by Eq. (25) (c) ρ_{nn} , after 50 NSMs for $\tau_2 = 2\tau_1$. (d) Same, after one CM with τ_3 that satisfies Eq. (28)

According to Eq. (24), each number state losses population to the number state that has one more photon via stimulated emission from the atom with probability $\sin^2(g\tau\sqrt{n+1})$. The outcome is a nonuniform drift of the Fock-state distribution towards increasing n . This drift is minimal for n that satisfy

$$g\tau\sqrt{n+1} \approx m\pi \quad (25)$$

for an integer m . When $g\tau$ and m are chosen to satisfy Eq. (25), the population of the corresponding $|n\rangle$ may grow at the expense of number states having smaller n , since Eq. (25) preclude photon emission. This $|n\rangle$ may be deemed a "trapping" state.

The populations of $|n\rangle$ in the range between consecutive states that satisfy the "trapping" condition are shifted as a results of an NSM that has the larger n . By iterating this shift, via multiple consecutive NSMs, one gradually concentrates the Fock-state distribution near the trapping states (Fig. 11). Yet, this concentration process is progressively slowed down, since the efficiency of shifting the distribution decreases for $|n\rangle$ near the i th trapping state $|n_i\rangle$. We can however accelerate the concentration upon reducing the atomic velocity by one half, thus doubling the traversal time τ and m in Eq. 25. The concentration process then regains its efficiency while keeping the velocity selection simple (Fig. 11).

2. Conditional measurements (CMs): NSMs alone cannot convert a thermal number-state distribution into a single number state, since they accumulate the number-state populations in the vicinity of several n values that satisfy the trapping

condition. As a remedy, we employ a “filter” based on a CM that erases portions of the distribution resort to near trapping states populated by the NSMs with the exception of number states we target. To this end, we send an atom in the excited state and measure whether, upon exiting the cavity, it is still in the excited state. The success probability is given by

$$P_e = \sum_{n=0}^{\infty} \rho_{nn} \cos^2(g\tau\sqrt{n+1}). \quad (26)$$

In this case the Fock-state populations are transformed as

$$\rho_{nn} \rightarrow P_e^{-1} \rho_{nn} \cos^2(g\tau\sqrt{n+1}). \quad (27)$$

If the CM fails, namely, we should resend another excited atom, and measure its state after it exits the cavity. Instead of Eq. (25), this CM requires

$$g\tau\sqrt{n+1} = (m + \frac{1}{2})\pi \quad (28)$$

so that the CM suppresses (“erases”!) the populations of Fock states near $|n\rangle$ for a chosen n and some integer m (Fig. 11).

A plausible experimental scenario starts from an initial thermal distribution of number states in the cavity, corresponding to the finite temperature of the cavity. The efficiency with which the field is transformed from such a broad thermal distribution to a very narrow distribution near the target Fock state is reflected by the Shannon entropy of the field,

$$S = - \sum_{n=0}^{\infty} \rho_{nn} \log \rho_{nn} \quad (29)$$

The Shannon entropy evolution allows us to monitor the entire preparation process (Fig. 12). It shows that by combining nonselective and conditional measurements (NSMs and CMs) on sequences of excited atoms sent through cavity, thermal high-entropy state can be transformed into a targeted number state with high probability after few measurements.

6 Discussion

We have surveyed the achievements and the potential of the recently introduced nonlinear (NL) thermodynamic effects in coherent, nondissipative systems, comparing the quantum and classical aspects of these effects. We have mostly dwelled on its conceivable implementation schemes and their technological prospects. The exploitation of NL intermode correlations for filtering or transforming thermal noise input into non-thermal output with controllable characteristics opens new perspectives for the realization of diverse thermodynamic devices with novel functionalities.

Apart from unconventional NL coherent heat engines [48], quantum microscopes [50] and quantum noise sensors [49] discussed in Sec. 2, other promising applications include NL quantum thermometers [111], as well as heat diodes and heat transistors [35–40] that may benefit from NL filtering of the thermal input.

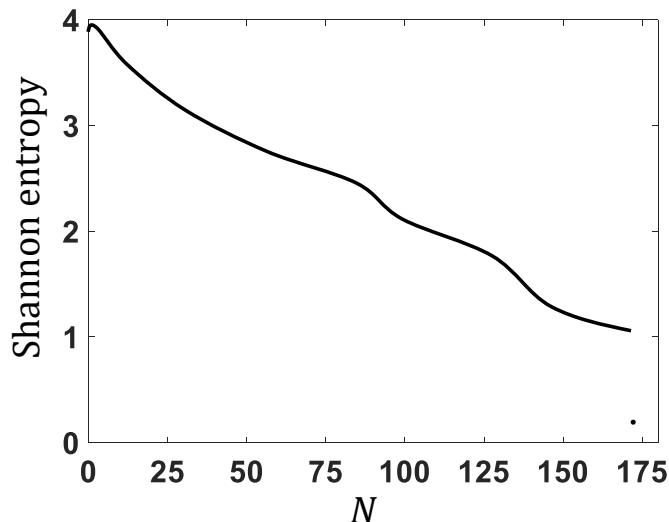


Fig. 12 Decreasing Shannon entropy of the output state in the cavity as a function of NSM numbers N in all the sequences completed by a successful CM.

A more ambitious, but not impossible, undertaking would be the construction of multi-node networks comprised of NL-coupled elements: such networks would be capable of performing classical calculations even with thermal input [91, 112]. Operation of NL coherent thermodynamic devices would not be prohibitively hard in the quantum domain, provided the goal is only to keep track of heat and ergotropy exchange between the modes, which are compatible with coarse graining of the evolution and are thus much less challenging than quantum computations that rely on multi-element entanglement [101] (Sec. 3). As we have shown, the salient quantum feature of thermal-noise NL filtering is the ability to control the output photon statistics and render the output state non-gaussian. The bottleneck impeding the realization of such NL thermodynamic devices is the need for giant nonlinearities that may yield large phase shifts of each evolving field mode by cross coupling it with only few quanta in other modes. At present, conversion of photons into dipole-dipole interacting Rydberg polaritons in a cold gas [82, 83] (Sec. 4) is the only demonstration of giant NL cross-Kerr effects between field modes populated by one or few photons. Dispersive field-atom interaction in an ultrahigh-Q cavity [90–92] can also exhibit a cross-Kerr effect with single photon per mode but cannot be readily incorporated in practical devices.

Yet, other promising technologies may be conceived with the goal of realizing few-photon NL devices:

- Multiatom interaction with fields in a moderately high-Q cavity: Since such a leaky cavity constitutes a photonic bath, its dispersive (off-resonant) interaction with multiple atoms is a realization of a scenario in which NL unitary effects, combined with dynamical control [89], transform an N -atom product state into a Schroedinger-cat state, alias GHZ or MQS state [84]. Subsequently, such a state can act as a massive entanglement resource that can transform two independent field modes

that interact with the cavity into an entangled two-mode N -photon state. (Sec.4). The feasibility of high-fidelity MQS entangled states with $N \leq 100$ may promote quantum sensing as well as one-way quantum computing [113].

- One may revisit the proposal for giant Kerr cross-coupling via interaction of a self-induced transparency (SIT) soliton in a resonantly-doped Bragg structure with a pulse subject to electromagnetically-induced transparency (EIT) [114]. Such an SIT soliton can have an arbitrarily small pulse area and slow velocity that matches the EIT-pulse velocity, so that the two pulses interact over long distances.
- As a substitute for the above deterministic, coherent approaches, one may employ probabilistic measurement-based state preparation that can emulate NL filtering of thermal noise. Such methods may include small-fraction photodetection (Sec. 5A) or homodyning measurements (Sec. 5B), which allow for thermal-state transformation into a non-Gaussian state conditioned on the measurement result, or the interaction of a thermal state in a cavity with a sequence of atoms which combines non-selective and conditional measurements, resulting in an output state that resembles a Fock state (Sec. 5C). Although the main goal of NL thermodynamics is to be the basis for coherent device operation, such “poor man’s” substitutes may have instructive merit and achieve similar device functionalities, at the price of dependence on the success or failure of the underlying measurements.
- As a curiosity, we note that the interaction of an atom with an empty cavity freely falling into a black hole can yield thermal photonic states, as if the cavity were immersed in a thermal bath, although both outside and inside the cavity there is complete vacuum [115]. The reason for such a paradoxical effect is the nonlinear transformation of the vacuum in the vicinity of a black hole. This transformation may also be classified as an exotic kind of NL thermodynamics.

To conclude, we hope that the nascent, unconventional theme of NL thermodynamics, which poses a broad range of intriguing conceptual and practical questions, will be further developed, both theoretically and experimentally. To this end, a variety of platforms and approaches may be harnessed, with a view of replacing the established paradigms of thermodynamic device composition and functionality by a new approach that emphasizes coherent, autonomous operation of such devices.

Data Availability Statement: No data associated in the manuscript.

Acknowledgements: G.K. and D.B.R.D. acknowledge support from the DFG under grant number FOR2724. A.M. acknowledges support from the Anusandhan National Research Foundation, Government of India, under grant number ANRF/E-CRG/2024/003836/PMS.

References

- [1] G. Kurizki, A.G. Kofman, *Thermodynamics and Control of Open Quantum Systems* (Cambridge University Press, 2022). <https://doi.org/10.1017/9781316798454>

- [2] F. Binder, L. Correa, C. Gogolin, J. Anders, G. Adesso, *Thermodynamics in the Quantum Regime: Fundamental Aspects and New Directions* (Springer, 2018)
- [3] H.E. Scovil, E.O. Schulz-DuBois, Three-level masers as heat engines. *Physical Review Letters* **2**(6), 262 (1959)
- [4] M.O. Scully, M.S. Zubairy, G.S. Agarwal, H. Walther, Extracting work from a single heat bath via vanishing quantum coherence. *Science* **299**(5608), 862–864 (2003). <https://doi.org/10.1126/science.1078955>. URL <https://science.sciencemag.org/content/299/5608/862>
- [5] M.O. Scully, K.R. Chapin, K.E. Dorfman, M.B. Kim, A. Svidzinsky, Quantum heat engine power can be increased by noise-induced coherence. *Proc. Natl. Acad. Sci.* **108**(37), 15097–15100 (2011). <https://doi.org/10.1073/pnas.1110234108>
- [6] J. Roßnagel, O. Abah, F. Schmidt-Kaler, K. Singer, E. Lutz, Nanoscale heat engine beyond the carnot limit. *Phys. Rev. Lett.* **112**, 030602 (2014). <https://doi.org/10.1103/PhysRevLett.112.030602>. URL <https://link.aps.org/doi/10.1103/PhysRevLett.112.030602>
- [7] W. Niedenzu, V. Mukherjee, A. Ghosh, A.G. Kofman, G. Kurizki, Quantum engine efficiency bound beyond the second law of thermodynamics. *Nature communications* **9**(1), 165 (2018)
- [8] L.M. Cangemi, C. Bhadra, A. Levy, Quantum engines and refrigerators. *Physics Reports* **1087**, 1–71 (2024)
- [9] A. Ghosh, C.L. Latune, L. Davidovich, G. Kurizki, Catalysis of heat-to-work conversion in quantum machines. *Proceedings of the National Academy of Sciences* **114**(46), 12156–12161 (2017). <https://doi.org/10.1073/pnas.1711381114>. URL <https://www.pnas.org/content/114/46/12156>
- [10] A. Ghosh, D. Gelbwaser-Klimovsky, W. Niedenzu, A.I. Lvovsky, I. Mazets, M.O. Scully, G. Kurizki, Two-level masers as heat-to-work converters. *Proceedings of the National Academy of Sciences* **115**(40), 9941–9944 (2018). <https://doi.org/10.1073/pnas.1805354115>. URL <https://www.pnas.org/content/115/40/9941>
- [11] A. Ferreri, H. Wang, F. Nori, F.K. Wilhelm, D.E. Bruschi, Quantum heat engine based on quantum interferometry: the su (1, 1) otto cycle. *arXiv preprint arXiv:2409.13411* (2024)
- [12] T. Guff, S. Daryanoosh, B.Q. Baragiola, A. Gilchrist, Power and efficiency of a thermal engine with a coherent bath. *Physical Review E* **100**(3), 032129 (2019)
- [13] M.O. Scully, Quantum photocell: Using quantum coherence to reduce radiative recombination and increase efficiency. *Physical review letters*

104(20), 207701 (2010)

- [14] K. Hammam, H. Leitch, Y. Hassouni, G. De Chiara, Exploiting coherence for quantum thermodynamic advantage. *New Journal of Physics* **24**(11), 113053 (2022)
- [15] J. Klaers, S. Faelt, A. Imamoglu, E. Togan, Squeezed thermal reservoirs as a resource for a nanomechanical engine beyond the carnot limit. *Physical Review X* **7**(3), 031044 (2017)
- [16] W. Niedenzu, D. Gelbwaser-Klimovsky, G. Kurizki, Performance limits of multi-level and multipartite quantum heat machines. *Physical Review E* **92**(4), 042123 (2015)
- [17] W. Niedenzu, G. Kurizki, Cooperative many-body enhancement of quantum thermal machine power. *New Journal of Physics* **20**(11), 113038 (2018)
- [18] A. Rolandi, P. Abiuso, M. Perarnau-Llobet, Collective advantages in finite-time thermodynamics. *Physical Review Letters* **131**(21), 210401 (2023)
- [19] J. Jaramillo, M. Beau, A. del Campo, Quantum supremacy of many-particle thermal machines. *New Journal of Physics* **18**(7), 075019 (2016)
- [20] A. Hartmann, V. Mukherjee, W. Niedenzu, W. Lechner, Many-body quantum heat engines with shortcuts to adiabaticity. *Physical Review Research* **2**(2), 023145 (2020)
- [21] F. Zhang, H. Quan, Work statistics across a quantum critical surface. *Physical Review E* **105**(2), 024101 (2022)
- [22] T. Fogarty, T. Busch, A many-body heat engine at criticality. *Quantum Science and Technology* **6**(1), 015003 (2020)
- [23] L.d.S. Souza, G. Manzano, R. Fazio, F. Iemini, Collective effects on the performance and stability of quantum heat engines. *Physical Review E* **106**(1), 014143 (2022)
- [24] R. B. S, V. Mukherjee, U. Divakaran, A. del Campo, Universal finite-time thermodynamics of many-body quantum machines from kibble-zurek scaling. *Physical Review Research* **2**(4), 043247 (2020)
- [25] J. Roßnagel, S.T. Dawkins, K.N. Tolazzi, O. Abah, E. Lutz, F. Schmidt-Kaler, K. Singer, A single-atom heat engine. *Science* **352**(6283), 325–329 (2016)
- [26] R. Kosloff, A. Levy, Quantum heat engines and refrigerators: Continuous devices. *Annu. Rev. Phys. Chem.* **65**(1), 365–393 (2014). <https://doi.org/10.1146/annurev-physchem-040513-103724>. URL <https://doi.org/10.1146/annurev-physchem-040513-103724>

- [27] R. Uzdin, A. Levy, R. Kosloff, Equivalence of quantum heat machines, and quantum-thermodynamic signatures. *Physical Review X* **5**(3), 031044 (2015)
- [28] R. Kosloff, A quantum mechanical open system as a model of a heat engine. *The Journal of chemical physics* **80**(4), 1625–1631 (1984)
- [29] A.E. Allahverdyan, R. Balian, T.M. Nieuwenhuizen, Maximal work extraction from finite quantum systems. *Europhysics Letters (EPL)* **67**(4), 565–571 (2004). <https://doi.org/10.1209/epl/i2004-10101-2>. URL <https://doi.org/10.1209/epl/i2004-10101-2>
- [30] M.T. Naseem, A. Misra, O.E. Müstecaplıoğlu, Two-body quantum absorption refrigerators with optomechanical-like interactions. *Quantum Science and Technology* **5**(3), 035006 (2020). <https://doi.org/10.1088/2058-9565/ab8d89>. URL <https://doi.org/10.1088/2058-9565/ab8d89>
- [31] B. Gardas, S. Deffner, Thermodynamic universality of quantum carnot engines. *Phys. Rev. E* **92**, 042126 (2015). <https://doi.org/10.1103/PhysRevE.92.042126>. URL <https://link.aps.org/doi/10.1103/PhysRevE.92.042126>
- [32] A. Misra, U. Singh, M.N. Bera, A.K. Rajagopal, Quantum rényi relative entropies affirm universality of thermodynamics. *Phys. Rev. E* **92**, 042161 (2015). <https://doi.org/10.1103/PhysRevE.92.042161>. URL <https://link.aps.org/doi/10.1103/PhysRevE.92.042161>
- [33] V. Mukherjee, A.G. Kofman, G. Kurizki, Anti-zeno quantum advantage in fast-driven heat machines. *Communications Physics* **3**(1), 8 (2020)
- [34] M. Xu, J. Stockburger, G. Kurizki, J. Ankerhold, Minimal quantum thermal machine in a bandgap environment: non-markovian features and anti-zeno advantage. *New journal of physics* **24**(3), 035003 (2022)
- [35] C. Kargi, M.T. Naseem, T. Opatrny, O.E. Müstecaplıoğlu, G. Kurizki, Quantum optical two-atom thermal diode. *Phys. Rev. E* **99**, 042121 (2019). <https://doi.org/10.1103/PhysRevE.99.042121>. URL <https://link.aps.org/doi/10.1103/PhysRevE.99.042121>
- [36] M.T. Naseem, A. Misra, O.E. Müstecaplıoğlu, G. Kurizki, Minimal quantum heat manager boosted by bath spectral filtering. *Phys. Rev. Research* **2**, 033285 (2020). <https://doi.org/10.1103/PhysRevResearch.2.033285>. URL <https://link.aps.org/doi/10.1103/PhysRevResearch.2.033285>
- [37] D. Segal, A. Nitzan, Spin-boson thermal rectifier. *Physical review letters* **94**(3), 034301 (2005)

- [38] O.P. Saira, M. Meschke, F. Giazotto, A.M. Savin, .f.M. Möttönen, J.P. Pekola, Heat transistor: Demonstration of gate-controlled electronic refrigeration. *Physical review letters* **99**(2), 027203 (2007)
- [39] D. Segal, Single mode heat rectifier: Controlling energy flow between electronic conductors. *Physical review letters* **100**(10), 105901 (2008)
- [40] Y. Shen, M. Bradford, J.T. Shen, Single-photon diode by exploiting the photon polarization in a waveguide. *Physical review letters* **107**(17), 173902 (2011)
- [41] N. Meher, S. Sivakumar, Atomic switch for control of heat transfer in coupled cavities. *Journal of the Optical Society of America B* **37**(1), 138–147 (2019)
- [42] B. Karimi, J. Pekola, M. Campisi, R. Fazio, Coupled qubits as a quantum heat switch. *Quantum Science and Technology* **2**(4), 044007 (2017)
- [43] A. Ronzani, B. Karimi, J. Senior, Y.C. Chang, J.T. Peltonen, C. Chen, J.P. Pekola, Tunable photonic heat transport in a quantum heat valve. *Nature Physics* **14**(10), 991–995 (2018)
- [44] K. Joulain, J. Drevillon, Y. Ezzahri, J. Ordóñez-Miranda, Quantum thermal transistor. *Physical review letters* **116**(20), 200601 (2016)
- [45] S. Das, A. Misra, A.K. Pal, A. Sen(De), U. Sen, Necessarily transient quantum refrigerator. *Euro Phys. Lett.* **125**(2), 20007 (2019). <https://doi.org/10.1209/0295-5075/125/20007>. URL <https://doi.org/10.1209/0295-5075/125/20007>
- [46] C. Mukhopadhyay, A. Misra, S. Bhattacharya, A.K. Pati, Quantum speed limit constraints on a nanoscale autonomous refrigerator. *Phys. Rev. E* **97**, 062116 (2018). <https://doi.org/10.1103/PhysRevE.97.062116>. URL <https://link.aps.org/doi/10.1103/PhysRevE.97.062116>
- [47] H.P. Breuer, F. Petruccione, *The theory of open quantum systems* (OUP Oxford, 2002)
- [48] T. Opatrný, Šimon Bräuer, A.G. Kofman, A. Misra, N. Meher, O. Firstenberg, E. Poem, G. Kurizki, Nonlinear coherent heat machines. *Science Advances* **9**(1), eadf1070 (2023). <https://doi.org/10.1126/sciadv.adf1070>. URL <https://www.science.org/doi/abs/10.1126/sciadv.adf1070>. <https://www.science.org/doi/pdf/10.1126/sciadv.adf1070>
- [49] N. Meher, T. Opatrný, G. Kurizki, Thermodynamic sensing of quantum nonlinear noise correlations. *Quantum Science and Technology* (2024)
- [50] N. Meher, E. Poem, T. Opatrný, O. Firstenberg, G. Kurizki, Supersensitive phase estimation by thermal light in a kerr-nonlinear interferometric setup. *Physical Review A* **110**(1), 013715 (2024)

- [51] G. Kurizki, N. Meher, T. Opatrny, Nonlinearity and quantumness in thermodynamics: From principles to technologies. *APL Quantum* **2**(1) (2025)
- [52] W. Pusz, S.L. Woronowicz, Passive states and kms states for general quantum systems. *Communications in Mathematical Physics* **58**, 273–290 (1978)
- [53] D. Gelbwaser-Klimovsky, G. Kurizki, Heat-machine control by quantum-state preparation: From quantum engines to refrigerators. *Phys. Rev. E* **90**, 022102 (2014). <https://doi.org/10.1103/PhysRevE.90.022102>. URL <https://link.aps.org/doi/10.1103/PhysRevE.90.022102>
- [54] S. Carnot, *Réflexions sur la puissance motrice du feu et sur les machines propres à développer cette puissance* (Bachelier Libraire, Paris, 1824)
- [55] R. Clausius, *The mechanical theory of heat* (Macmillan, 1879)
- [56] C. Han, D. Cohen, E. Sela, Quantum limitation on experimental testing of nonequilibrium fluctuation theorems. *Physical Review B* **110**(11), 115153 (2024)
- [57] C. Han, N. Katz, E. Sela, Prospect for measuring work statistics in quantum coherent systems. *arXiv preprint arXiv:2503.20729* (2025)
- [58] C. Gerry, P.L. Knight, *Introductory Quantum Optics* (Cambridge University Press, 2004)
- [59] H.F. Hofmann, All path-symmetric pure states achieve their maximal phase sensitivity in conventional two-path interferometry. *Phys. Rev. A* **79**, 033822 (2009). <https://doi.org/10.1103/PhysRevA.79.033822>. URL <https://link.aps.org/doi/10.1103/PhysRevA.79.033822>
- [60] M. Kitagawa, M. Ueda, Squeezed spin states. *Physical Review A* **47**(6), 5138 (1993)
- [61] T. Opatrny, Twisting tensor and spin squeezing. *Physical Review A* **91**(5), 053826 (2015)
- [62] T. Opatrny, Squeezing with classical hamiltonians. *Physical Review A* **92**(3), 033801 (2015)
- [63] N. Cottet, S. Jezouin, L. Bretheau, P. Campagne-Ibarcq, Q. Ficheux, J. Anders, A. Auffèves, R. Azouit, P. Rouchon, B. Huard, Observing a quantum maxwell demon at work. *Proceedings of the National Academy of Sciences* **114**(29), 7561–7564 (2017)
- [64] H. Carmichael, *Statistical Methods in Quantum Optics* (Springer, Berlin, 1999)
- [65] C.W. Gardiner, P. Zoller, *Quantum Noise* (Springer, Berlin, 2000)

- [66] M.O. Scully, M.S. Zubairy, *Quantum Optics* (Cambridge University Press, 2012)
- [67] I. Afek, O. Ambar, Y. Silberberg, Classical bound for mach-zehnder super-resolution. *Phys. Rev. Lett.* **104**, 123602 (2010). <https://doi.org/10.1103/PhysRevLett.104.123602>. URL <https://link.aps.org/doi/10.1103/PhysRevLett.104.123602>
- [68] A. Monras, Optimal phase measurements with pure gaussian states. *Phys. Rev. A* **73**, 033821 (2006). <https://doi.org/10.1103/PhysRevA.73.033821>. URL <https://link.aps.org/doi/10.1103/PhysRevA.73.033821>
- [69] O. Pinel, P. Jian, N. Treps, C. Fabre, D. Braun, Quantum parameter estimation using general single-mode gaussian states. *Phys. Rev. A* **88**, 040102 (2013). <https://doi.org/10.1103/PhysRevA.88.040102>. URL <https://link.aps.org/doi/10.1103/PhysRevA.88.040102>
- [70] S. Boixo, S.T. Flammia, C.M. Caves, J. Geremia, Generalized limits for single-parameter quantum estimation. *Phys. Rev. Lett.* **98**, 090401 (2007). <https://doi.org/10.1103/PhysRevLett.98.090401>. URL <https://link.aps.org/doi/10.1103/PhysRevLett.98.090401>
- [71] V. Giovannetti, S. Lloyd, L. Maccone, Quantum measurement bounds beyond the uncertainty relations. *Phys. Rev. Lett.* **108**, 260405 (2012). <https://doi.org/10.1103/PhysRevLett.108.260405>. URL <https://link.aps.org/doi/10.1103/PhysRevLett.108.260405>
- [72] H. Cramér, *Mathematical methods of statistics*, vol. 43 (Princeton university press, 1999)
- [73] R.J. Birrittella, P.M. Alsing, C.C. Gerry, The parity operator: Applications in quantum metrology. *AVS Quantum Science* **3**(1) (2021). <https://doi.org/10.1116/5.0026148>. URL <https://doi.org/10.1116/5.0026148>
- [74] I.L. Chuang, M.A. Nielsen, Prescription for experimental determination of the dynamics of a quantum black box. *Journal of Modern Optics* **44**(11-12), 2455–2467 (1997)
- [75] N. Goldman, J. Dalibard, Periodically driven quantum systems: Effective hamiltonians and engineered gauge fields. *Phys. Rev. X* **4**, 031027 (2014). <https://doi.org/10.1103/PhysRevX.4.031027>. URL <https://link.aps.org/doi/10.1103/PhysRevX.4.031027>
- [76] J. Del Pino, O. Zilberberg, Dynamical gauge fields with bosonic codes. *Physical Review Letters* **130**(17), 171901 (2023)
- [77] M. Mohseni, A.T. Rezakhani, D.A. Lidar, Quantum-process tomography: Resource analysis of different strategies. *Phys. Rev. A* **77**, 032322 (2008).

<https://doi.org/10.1103/PhysRevA.77.032322>. URL <https://link.aps.org/doi/10.1103/PhysRevA.77.032322>

- [78] A.I. Lvovsky, M.G. Raymer, Continuous-variable optical quantum-state tomography. *Rev. Mod. Phys.* **81**, 299–332 (2009). <https://doi.org/10.1103/RevModPhys.81.299>. URL <https://link.aps.org/doi/10.1103/RevModPhys.81.299>
- [79] R. Uzdin, S. Rahav, Global passivity in microscopic thermodynamics. *Physical Review X* **8**(2), 021064 (2018)
- [80] D. Varshalovich, *Quantum theory of angular momentum*
- [81] U. Leonhardt, *Measuring the quantum state of light*, vol. 22 (Cambridge university press, 1997)
- [82] I. Friedler, D. Petrosyan, M. Fleischhauer, G. Kurizki, Long-range interactions and entanglement of slow single-photon pulses. *Phys. Rev. A* **72**, 043803 (2005). <https://doi.org/10.1103/PhysRevA.72.043803>. URL <https://link.aps.org/doi/10.1103/PhysRevA.72.043803>
- [83] L. Drori, B.C. Das, T.D. Zohar, G. Winer, E. Poem, A. Poddubny, O. Firstenberg, Quantum vortices of strongly interacting photons. *Science* **381**(6654), 193–198 (2023)
- [84] D. Bhaktavatsala Rao, N. Bar-Gill, G. Kurizki, Generation of macroscopic superpositions of quantum states by linear coupling to a bath. *Physical review letters* **106**(1), 010404 (2011)
- [85] C. Cohen-Tannoudji, J. Dupont-Roc, G. Grynberg, *Atom-photon interactions: basic processes and applications* (John Wiley & Sons, 1998)
- [86] B. Yurke, D. Stoler, Generating quantum mechanical superpositions of macroscopically distinguishable states via amplitude dispersion. *Physical review letters* **57**(1), 13 (1986)
- [87] I. Schuster, A. Kubanek, A. Fuhrmanek, T. Puppe, P.W. Pinkse, K. Murr, G. Rempe, Nonlinear spectroscopy of photons bound to one atom. *Nature Physics* **4**(5), 382–385 (2008)
- [88] D. Braun, Creation of entanglement by interaction with a common heat bath. *Physical Review Letters* **89**(27), 277901 (2002)
- [89] J. Clausen, G. Bentsky, G. Kurizki, Bath-optimized minimal-energy protection of quantum operations from decoherence. *Physical review letters* **104**(4), 040401 (2010)

- [90] H. Walther, B.T. Varcoe, B.G. Englert, T. Becker, Cavity quantum electrodynamics. *Reports on Progress in Physics* **69**(5), 1325 (2006)
- [91] A. Reiserer, G. Rempe, Cavity-based quantum networks with single atoms and optical photons. *Reviews of Modern Physics* **87**(4), 1379–1418 (2015)
- [92] N. Meher, S. Sivakumar, A review on quantum information processing in cavities. *The European Physical Journal Plus* **137**(8), 985 (2022). <https://doi.org/10.1140/epjp/s13360-022-03172-x>. URL <https://doi.org/10.1140/epjp/s13360-022-03172-x>
- [93] A. Dantan, M. Pinard, Quantum-state transfer between fields and atoms in electromagnetically induced transparency. *Physical Review A—Atomic, Molecular, and Optical Physics* **69**(4), 043810 (2004)
- [94] D.B.R. Dasari, S. Yang, A. Chakrabarti, A. Finkler, G. Kurizki, J. Wrachtrup, Anti-zeno purification of spin baths by quantum probe measurements. *Nature communications* **13**(1), 7527 (2022)
- [95] A. Kofman, G. Kurizki, Acceleration of quantum decay processes by frequent observations. *Nature* **405**(6786), 546–550 (2000)
- [96] S. Virzì, A. Avella, F. Piacentini, M. Gramegna, T. Opatrný, A.G. Kofman, G. Kurizki, S. Gherardini, F. Caruso, I.P. Degiovanni, et al., Quantum zeno and anti-zeno probes of noise correlations in photon polarization. *Physical review letters* **129**(3), 030401 (2022)
- [97] A. Misra, T.c.v. Opatrný, G. Kurizki, Work extraction from single-mode thermal noise by measurements: How important is information? *Phys. Rev. E* **106**, 054131 (2022). <https://doi.org/10.1103/PhysRevE.106.054131>. URL <https://link.aps.org/doi/10.1103/PhysRevE.106.054131>
- [98] T. Opatrný, A. Misra, G. Kurizki, Work generation from thermal noise by quantum phase-sensitive observation. *Phys. Rev. Lett.* **127**, 040602 (2021). <https://doi.org/10.1103/PhysRevLett.127.040602>. URL <https://link.aps.org/doi/10.1103/PhysRevLett.127.040602>
- [99] T. Sagawa, M. Ueda, Second law of thermodynamics with discrete quantum feedback control. *Phys. Rev. Lett.* **100**(8), 080403 (2008)
- [100] M.D. Vidrighin, O. Dahlsten, M. Barbieri, M.S. Kim, V. Vedral, I.A. Walmsley, Photonic Maxwell’s demon. *Phys. Rev. Lett.* **116**, 050401 (2016). <https://doi.org/10.1103/PhysRevLett.116.050401>. URL <https://link.aps.org/doi/10.1103/PhysRevLett.116.050401>
- [101] M. Nielsen, I. Chuang, *Quantum Computation and Quantum Information* (Cambridge University Press, Cambridge, UK, 2000)

- [102] W. Niedenzu, V. Mukherjee, A. Ghosh, A.G. Kofman, G. Kurizki, Quantum engine efficiency bound beyond the second law of thermodynamics. *Nature Communications* **9**(1), 165 (2018). <https://doi.org/10.1038/s41467-017-01991-6>. URL <https://doi.org/10.1038/s41467-017-01991-6>
- [103] J. Yi, P. Talkner, Y.W. Kim, Single-temperature quantum engine without feedback control. *Phys. Rev. E* **96**, 022108 (2017). <https://doi.org/10.1103/PhysRevE.96.022108>. URL <https://link.aps.org/doi/10.1103/PhysRevE.96.022108>
- [104] N. Erez, G. Gordon, M. Nest, G. Kurizki, Thermodynamic control by frequent quantum measurements. *Nature* **452**(7188), 724–727 (2008). <https://doi.org/10.1038/nature06873>. URL <https://doi.org/10.1038/nature06873>
- [105] D. Gelbwaser-Klimovsky, N. Erez, R. Alicki, G. Kurizki, Work extraction via quantum nondemolition measurements of qubits in cavities: Non-markovian effects. *Phys. Rev. A* **88**, 022112 (2013). <https://doi.org/10.1103/PhysRevA.88.022112>. URL <http://link.aps.org/doi/10.1103/PhysRevA.88.022112>
- [106] R. Landauer, Irreversibility and heat generation in the computing process. *IBM Journal of Research and Development* **5**(3), 183–191 (1961)
- [107] G. Harel, G. Kurizki, Fock-state preparation from thermal cavity fields by measurements on resonant atoms. *Physical Review A* **54**(6), 5410 (1996)
- [108] A. Kozhekin, G. Kurizki, B. Sherman, Quantum-state control by a single conditional measurement: The periodically switched jaynes-cummings model. *Physical Review A* **54**(4), 3535 (1996)
- [109] G. Harel, G. Kurizki, J. McIver, E. Coutsias, Optimized preparation of quantum states by conditional measurements. *Physical Review A* **53**(6), 4534 (1996)
- [110] B.M. Garraway, B. Sherman, H. Moya-Cessa, P.L. Knight, G. Kurizki, Generation and detection of nonclassical field states by conditional measurements following two-photon resonant interactions. *Phys. Rev. A* **49**, 535–547 (1994). <https://doi.org/10.1103/PhysRevA.49.535>. URL <https://link.aps.org/doi/10.1103/PhysRevA.49.535>
- [111] V. Mukherjee, A. Zwick, A. Ghosh, X. Chen, G. Kurizki, Enhanced precision bound of low-temperature quantum thermometry via dynamical control. *Communications Physics* **2**(1), 162 (2019)
- [112] J.L. Miller, Nonlinear optical computing doesn’t need nonlinear optics. *Physics Today* **77**(10), 12–14 (2024)
- [113] H.J. Briegel, D.E. Browne, W. Dür, R. Raussendorf, M. Van den Nest, Measurement-based quantum computation. *Nature Physics* **5**(1), 19–26 (2009)

- [114] G. Kurizki, D. Petrosyan, T. Opatrny, M. Blaauboer, B. Malomed, Nonlinear optics of photonic crystals-enhanced nonlinear optics with photonic crystals-self-induced transparency and giant nonlinearity in doped photonic crystals. *Journal of the Optical Society of America-B-Optical Physics* **19**(9), 2066–2074 (2002)
- [115] A. Misra, P. Chattopadhyay, A. Svidzinsky, M.O. Scully, G. Kurizki, Black-hole powered quantum coherent amplifier. *npj Quantum Information* **10**(1), 34 (2024)